October 6, 2010

Calibration of the Total Carbon Column Observing Network Using Aircraft Profile Data

D. Wunch, *California Institute of Technology*
G. C. Toon, *California Institute of Technology*
P. O. Wennberg, *California Institute of Technology*
Steven C. Wofsy, *Harvard University*
B. B. Stephens, *National Center for Atmospheric Research*, et al.

Atmos. Meas. Tech., 3, 1351–1362, 2010
www.atmos-meas-tech.net/3/1351/2010/
doi:10.5194/amt-3-1351-2010

Atmospheric Measurement Techniques

Calibration of the Total Carbon Column Observing Network using aircraft profile data

D. Wunch[1], G. C. Toon[2,1], P. O. Wennberg[1], S. C. Wofsy[3], B. B. Stephens[4], M. L. Fischer[10], O. Uchino[14], J. B. Abshire[12], P. Bernath[8,9], S. C. Biraud[10], J.-F. L. Blavier[2,1], C. Boone[8], K. P. Bowman[13], E. V. Browell[11], T. Campos[4], B. J. Connor[7], B. C. Daube[3], N. M. Deutscher[5], M. Diao[15], J. W. Elkins[17], C. Gerbig[16], E. Gottlieb[3], D. W. T. Griffith[5], D. F. Hurst[18,17], R. Jiménez[3,21], G. Keppel-Aleks[1], E. A. Kort[3], R. Macatangay[5], T. Machida[14], H. Matsueda[19], F. Moore[18], I. Morino[14], S. Park[3], J. Robinson[20], C. M. Roehl[1], Y. Sawa[19], V. Sherlock[6], C. Sweeney[18], T. Tanaka[14], and M. A. Zondlo[15]

[1]California Institute of Technology, Pasadena, CA, USA
[2]Jet Propulsion Laboratory, California Institute of Technology, Pasadena, CA, USA
[3]Harvard University, Cambridge, MA, USA
[4]National Center for Atmospheric Research, Boulder, CO, USA
[5]Center for Atmospheric Chemistry, University of Wollongong, Wollongong, NSW, Australia
[6]National Institute of Water & Atmospheric Research, Wellington, New Zealand
[7]BC Consulting Limited, Alexandra, New Zealand
[8]University of Waterloo, Waterloo, ON, Canada
[9]York University, York, UK
[10]Lawrence Berkeley National Laboratories, Berkeley, CA, USA
[11]NASA Langley Research Center, Hampton, VA, USA
[12]NASA Goddard Space Flight Center, Greenbelt, MD, USA
[13]Texas A&M University, College Station, TX, USA
[14]National Insitute for Environmental Studies, Tsukuba, Japan
[15]Princeton University, Princeton, NJ, USA
[16]Max-Planck-Institut für Biogeochemie, Jena, Germany
[17]National Oceanic and Atmospheric Administration, Boulder, CO, USA
[18]Cooperative Institute for Research in Environmental Sciences, University of Colorado, Boulder, CO, USA
[19]Meteorological Research Institute, Tsukuba, Japan
[20]National Institute of Water & Atmospheric Research, Lauder, New Zealand
[21]Department of Chemical and Enivronmental Engineering, Universidad Nacional de Colombia, Bogota, DC 111321, Colombia

Received: 27 May 2010 – Published in Atmos. Meas. Tech. Discuss.: 17 June 2010
Revised: 16 September 2010 – Accepted: 17 September 2010 – Published: 6 October 2010

Abstract. The Total Carbon Column Observing Network (TCCON) produces precise measurements of the column average dry-air mole fractions of CO_2, CO, CH_4, N_2O and H_2O at a variety of sites worldwide. These observations rely on spectroscopic parameters that are not known with sufficient accuracy to compute total columns that can be used in combination with in situ measurements. The TCCON must therefore be calibrated to World Meteorological Organization (WMO) in situ trace gas measurement scales. We present a calibration of TCCON data using WMO-scale instrumentation aboard aircraft that measured profiles over four TCCON stations during 2008 and 2009. These calibrations are compared with similar observations made in 2004 and 2006. The results indicate that a single, global calibration factor for each gas accurately captures the TCCON total column data within error.

Correspondence to: D. Wunch
(dwunch@gps.caltech.edu)

Published by Copernicus Publications on behalf of the European Geosciences Union.

1 Introduction

The Total Carbon Column Observing Network (TCCON) is a ground-based network of Fourier transform spectrometers that precisely measure total columns of CO_2, CO, CH_4, N_2O, H_2O, HF and other gases (Wunch et al., 2010). The TCCON instruments measure the absorption of direct sunlight by atmospheric gases in the near infrared (NIR) spectral region. To derive a total column measurement of the gases from these spectra, external information about the atmosphere (e.g. temperature, pressure, a priori mixing ratio) and NIR spectroscopy is required. A significant effort is put into minimizing errors in this external information, and the resulting total columns are precise (e.g. <0.25% in CO_2).

Due to systematic biases in the spectroscopy, the absolute accuracy of the column measurements is ∼1%, which is inadequate for use in combination with in situ measurements for carbon cycle science. In order to make TCCON column measurements useful for these combined analyses, they must be calibrated to the World Meteorological Organization (WMO) in situ trace gas measurement scales. To do this, we use profiles obtained with in situ instrumentation flown on aircraft over TCCON sites. A set of profiles were measured over the Park Falls, Wisconsin TCCON site in 2004–2005 (Washenfelder et al., 2006) during the Intercontinental Chemical Transport Experiment–North America campaign (INTEX-NA, Singh et al., 2006) and the CO_2 Budget and Rectification Airborne – Maine experiment (COBRA-ME, Gerbig et al., 2003; Lin et al., 2006). A single profile was measured coincidently with the Darwin, Australia site in 2006 as part of the Tropical Warm Pool International Cloud Experiment (TWP-ICE, Deutscher et al., 2010; May et al., 2008). Since then, other TCCON sites have begun operational measurements. In this paper, we describe the first global calibration of five TCCON sites (Park Falls, Lamont, Darwin, Lauder and Tsukuba), using instrumentation calibrated to WMO scales aboard the HIAPER aircraft, during the START-08 and HIPPO overpasses in 2008 and 2009, Learjet overflights of Lamont in 2009, and a Beechcraft King Air 200T aircraft profile over Tsukuba, Japan in 2009 (Tanaka et al., 2009). We present the calibration of CO_2, CO, CH_4, N_2O and H_2O.

2 TCCON

The TCCON was developed to provide a long, nearly continuous time series to serve as a transfer standard between in situ networks and satellite measurements, and to provide insights into the carbon cycle (e.g., Yang et al., 2007; Keppel-Aleks et al., 2008; Wunch et al., 2009; Deutscher et al., 2010). TCCON sites are located worldwide (Fig. 1). The first TCCON site, located in Park Falls, is described by Washenfelder et al. (2006).

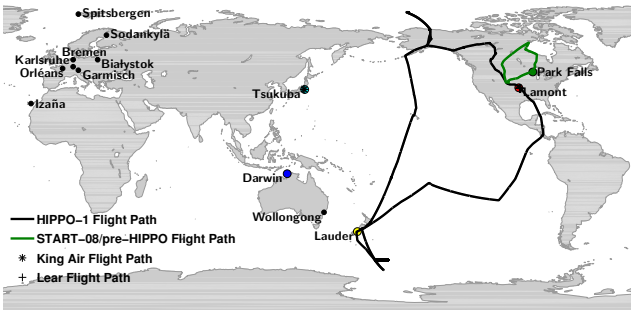

Fig. 1. TCCON site locations. The HIPPO flight path is overlaid in solid black, START-08 in solid green. The King Air flight path is marked by black stars (*) directly over the Tsukuba site, and the Lear flight path is marked in black plusses (+) directly over the Lamont site.

Table 1. TCCON spectral windows and spectroscopy. If a single molecule is retrieved in multiple windows, the results are averaged. References are 1, Rothman et al. (2009); 1[a], Rothman et al. (2009, November update); 2, Toth et al. (2008); 3, Frankenberg et al. (2008); 4, Smith and Newnham (2000); 5, Yang et al. (2005); 6, Gordon et al. (2010); 7, Toth (2005); 8, Jenouvrier et al. (2007).

Molecule	Central wavenumber (cm^{-1})	Spectral width (cm^{-1})	Spectroscopic line list
CO_2	6220.00	80.00	1, 2
	6339.50	85.00	1, 2
CO	4233.00	48.60	1
	4290.40	56.80	1
CH_4	5938.00	116.00	1, 3
	6002.00	11.10	1, 3
	6076.00	138.00	1, 3
N_2O	4395.50	37.70	1
	4429.80	23.60	1
O_2	7885.00	240.00	1[a], 4, 5, 6
HF	4038.95	0.32	1
H_2O	6076.90	3.85	1, 7, 8
	6099.35	0.95	1, 7, 8
	6125.85	1.45	1, 7, 8
	6177.30	0.83	1, 7, 8
	6255.95	3.60	1, 7, 8
	6301.35	7.90	1, 7, 8
	6392.45	3.10	1, 7, 8
	6401.15	1.15	1, 7, 8
	6469.60	3.50	1, 7, 8

Total column abundances are retrieved from spectra measured with the TCCON instruments using a nonlinear least-squares spectral fitting algorithm (GFIT), which scales an a priori profile to produce a synthetic spectrum that achieves the best fit to the measured spectrum. We use the spectral windows and spectroscopic data listed in Table 1.

Table 2. Aircraft instrumentation used in this study. Demonstrated in-flight precision and estimated accuracy for each instrument and molecule are listed in column 4.

Flight	Instrument	Species	Precision, Accuracy	Notes
HIPPO	HAIS/Harvard Quantum Cascade Laser Spectrometer (QCLS)	CO_2	0.02 ppm, 0.1 ppm	1 s, 1σ precision; 1σ accuracy
		CH_4	0.5 ppb, 1 ppb	1 s, 1σ precision; 1σ accuracy
		CO	0.15 ppb, 3.5 ppb	1 s, 1σ precision; 1σ accuracy
		N_2O	0.09 ppb, 0.2 ppb	1 s, 1σ precision; 1σ accuracy
	Harvard OMS	CO_2	0.1 ppm, 0.1 ppm	1 s, 1σ precision; 1σ accuracy
	NCAR Airborne Oxygen (AO2) Li-840	CO_2	0.3 ppm, 0.1 ppm	10 s, 1σ precision; long-term (>1 min) 1σ accuracy
	NCAR Research Aviation Facility (RAF)	CO	2 ppb, $\pm$ 2 ppb + 5%	10 s, 1σ precision; 1σ accuracy
	HAIS/Princeton Vertical Cavity Surface Emitting Laser Hygrometer (VCSEL)	H_2O	<3%, 5%	1 s, 1σ precision
START-08/ pre-HIPPO	HAIS/Harvard Quantum Cascade Laser Spectrometer (QCLS)	CO_2	0.16 ppm, 0.16 ppm	10 s, 1σ precision; 1σ accuracy
		CH_4	4.5 ppb, 4.5 ppb	10 s, 1σ precision; 1σ accuracy
		CO	1.3 ppb, 3.5 ppb	10 s, 1σ precision; 1σ accuracy
		N_2O	0.7 ppb, 0.7 ppb	10 s, 1σ precision; 1σ accuracy
	NCAR Airborne Oxygen (AO2) Li-840	CO_2	0.3 ppm, 0.1 ppm	10 s, 1σ precision; long-term (>1 min) 1σ accuracy
	NCAR Research Aviation Facility (RAF)	CO	2 ppb, $\pm$ 2 ppb + 5%	10 s, 1σ precision; 1σ accuracy
	HAIS/Princeton Vertical Cavity Surface Emitting Laser Hygrometer (VCSEL)	H_2O	<3%, 5%	1 s, 1σ precision
	NOAA Unmanned Aircraft Systems Chromatograph for Atmospheric Trace Species (UCATS)	CH_4	13 ppb, <13 ppb	1σ precision and accuracy
		H_2O	5%,7%	1σ precision
Learjet	NOAA Flask Samplers	CO_2	0.03 ppm, 0.155 ppm	1σ for 12 flasks (~28 day) precision and accuracy
		CH_4	1.2 ppb, 1.06 ppb	1σ for 12 flasks (~28 day) precision and accuracy
		CO	0.3 ppb, 0.8 ppb	1σ for 12 flasks (~28 day) precision and accuracy
		N_2O	0.4 ppb, 0.3 ppb	1σ for 12 flasks (~28 day) precision and accuracy
Beechcraft King Air 200T	CO_2 Continuous Measurement Equipment (CME) Li-COR 840 non-dispersive infrared analyser	CO_2	0.2 ppm, 0.12 $\pm$ 0.02 ppm	10 s, 1.645σ (90%) precision; 1σ accuracy
	Hand-operated Flask Sampling Equipment (HSE)	CH_4	1.7 ppb, 4.1 $\pm$ 0.6 ppb	1σ precision and accuracy
COBRA-ME	Harvard OMS	CO_2	0.1 ppm, 0.1 ppm	1 s, 1σ precision; 1σ accuracy
	Harvard Aerolaser VUV	CO	2 ppb, $\pm$ 3 ppb + 3%	1 s, 1σ precision; 1σ accuracy
INTEX-NA	LI-COR 6252	CO_2	0.1 ppm, $\pm$0.25 ppm	1 s, 1σ precision; 1σ accuracy
	UCI Grab samples analyzed with GC and GC/MS	CH_4	$\pm$0.1%, 1%	1σ precision; 1σ accuracy
TWP-ICE	Harvard OMS	CO_2	0.1 ppm, 0.1 ppm	1 s, 1σ precision; 1σ accuracy

Column-averaged dry-air mole fractions (DMF), denoted X_G for gas G, are computed using the retrieved O_2 columns as a measure of the dry air column.

$$X_G = 0.2095 \frac{\text{column}_G}{\text{column}_{O_2}} \quad (1)$$

Dividing by O_2 improves the precision of the measurement by significantly reducing the effects of instrumental or measurement errors that are common to both the gases (e.g. solar tracker pointing errors, zero level offsets, instrument line shape errors, etc. described in Wunch et al., 2010). However, any errors specific to either column_G or column_{O_2} will create errors in the DMFs of each gas.

Atmospheric O_2 is not, as assumed by GFIT, constant. The seasonal cycle in the O_2/N_2 ratio ranges globally by ~10–30 ppm of O_2 (Bender et al., 1998), peaking in the summer, when the CO_2 amounts are at their minimum. Using a constant O_2 amount overestimates the seasonal cycle in X_{CO_2} by ~0.05 ppm. The long-term depletion of O_2 is about twice the rate of the atmospheric CO_2 increase (Tohjima et al., 2005; Bender et al., 1998). Assuming a ~2 ppm annual CO_2 increase, GFIT will overestimate the secular increase by ~0.4%, or ~0.01 ppm X_{CO_2}/year. This small time-dependence will be built into a future version of our processing algorithm.

All TCCON X_{CO_2} data have an airmass-dependent artifact, which causes the retrievals to be ~1% larger at low solar zenith angles than at high solar zenith angles (Wunch et al., 2010). This artifact is caused primarily by spectroscopic inadequacies which are common to all TCCON instruments (e.g. line widths, neglect of line-mixing, inconsistencies in the relative strengths of weak and strong lines). The airmass-dependent artifact is removed from the TCCON data with a single empirical correction factor before calibration. Airmass dependent artifacts have not been seen in X_{CH_4}, X_{CO}, X_{N_2O} or X_{H_2O}.

For comparison with the aircraft profiles, which are not measured instantaneously, averages are taken of TCCON X_{CO_2}, X_{CH_4}, X_{CO}, and X_{N_2O} columns retrieved while the aircraft measurements were taking place, weather permitting. Typical durations are between 0.5–4 h. The standard deviations (1σ) of the measurements are taken as the TCCON errors. One hour of TCCON measurements of X_{H_2O} are averaged to compare with each sonde profile, centered on the

sonde launch time. Twice the standard deviations (2σ) of the X_{H_2O} measurements are taken as the TCCON errors, because the atmospheric variability of H_2O can be much greater than for the other molecules (Sussmann et al., 2009).

3 Aircraft campaigns

Three independent aircraft campaigns were held in 2008 and 2009 that included profiles over four TCCON stations. The instrumentation on each aircraft used for the calibration are listed in Table 2, and the dates of the profiles over TCCON sites are listed in Table 3. The WMO calibration scales used for the aircraft instrumentation are described for CO_2 in Zhao and Tans (2006) and Keeling et al. (2002), for N_2O in Hall et al. (2007), for CH_4 in Dlugokencky et al. (2005) and for CO in Novelli et al. (1994). Demonstrated precision and accuracy for each instrument and each molecule are listed in Table 2.

3.1 START-08/pre-HIPPO and HIPPO-1

The NCAR/NSF High-performance Instrumented Airborne Platform for Environmental Research (HIAPER), is a modified Gulfstream V (GV) jet which hosted the Stratosphere-Troposphere Analyses of Regional Transport 2008 (START-08) campaign (Pan et al., 2010) and the preliminary HIAPER Pole-to-Pole Observations (pre-HIPPO) campaign during 2008. The two campaigns shared flight time and instrumentation and made observations across North America, including a vertical profile above the Park Falls site in May, 2008. The HIAPER Pole-to-Pole Observations (HIPPO-1) campaign (Wofsy et al., 2010) covered a cross-section of the globe that spanned the Arctic to the Antarctic (Fig. 1) with profiles over Lamont and Lauder in January, 2009. The START-08/pre-HIPPO and HIPPO-1 missions used similar in situ instrumentation (Table 2). The water profiles are from the available H_2O measurements on board the aircraft (e.g., VCSEL: Zondlo et al., 2010), with additional stratospheric information supplied by the noontime NCEP/NCAR specific humidity profile for that day. The HIPPO-1 profiles used in this analysis over Lamont are shown in Fig. 2.

3.2 Learjet

The NASA Glenn Lear-25 aircraft performed three profiles from 5–13 km altitude over the Southern Great Plains (SGP) Atmospheric Radiation Measurement (ARM) Lamont site during a campaign from 31 July 2009 to 5 August 2009 (Abshire et al., 2010). Lower altitude (0.3–5 km) profiles were measured with a Cessna 210 at essentially the same times and locations. On both aircraft, the CO_2, CH_4, N_2O and CO measurements were made by flask samplers, which were analysed at the National Oceanic and Atmospheric Administration's Earth System Research Laboratory (NOAA's ESRL). Precisions and accuracies listed in Table 2 for the NOAA Flask Samplers are from Ness et al. (2010) (http://www.esrl.noaa.gov/gmd/ccgg/aircraft/qc.html). Water profiles were obtained from on-site sonde measurements taken at 11:30 a.m. LT.

Many years of bi-weekly Cessna 0–5 km flights are also available over Park Falls and Lamont and will be used in a future analysis to assess possible calibration drifts for those sites. The ceiling of these flights is insufficiently high for use in this analysis.

3.3 Beechcraft King Air

The Beechcraft King Air 200T aircraft measures CO_2 continuously with a Li-COR (Li-840) non-dispersive infrared analyzer. CH_4 and other gases are measured using hand-operated flask samplers, which are analysed at the National Institute for Environmental Studies (NIES). Precisions and accuracies for the Beechcraft King Air instrumentation listed in Table 2 are from Machida et al. (2008), Machida et al. (2007) and Zhou et al. (2009).

The aircraft overpasses of the Tsukuba FTS instrument were carried out on 7 and 15 January 2009 over Tsukuba (36.1° N, 140.1° E) and Kumagaya (36.15° N, 139.38° E). Due to air traffic control restrictions, the higher part of the profile (2 to 7 km) was observed over Kumagaya, and the lower altitude range (0.5 to 2 km) was observed over Tsukuba. For the purposes of the FTS calibration, only data from the 15 January overflight is used, because of heavy cloud cover on 7 January. Water profiles were obtained from nearby radiosonde measurements taken at the Tateno Aerological Observatory near the time of the overpass.

4 Numerical integration of aircraft in situ profiles

To calibrate the total column measurements of the TCCON network, the aircraft in situ profiles must be integrated with respect to altitude. In order to properly compare the ground-based FTS measurements with the in situ aircraft measurement, which we consider the best measure of the true state of the atmosphere, the averaging kernels of the FTS measurements ($\mathbf{A}$) must be taken into account. From the aircraft profiles ($\boldsymbol{x_h}$), an averaging kernel-smoothed profile ($\boldsymbol{x_s}$) can be computed that, when integrated, can be directly compared with the FTS retrieved total columns. The smoothed profile represents the profile that should be retrieved, if the FTS were measuring the true atmospheric profile without spectroscopic errors, given the GFIT a priori profile ($\boldsymbol{x_a}$) and retrieved profile scale factor (γ). We use Eq. (4) of Rodgers and Connor (2003),

$$\boldsymbol{x_s} = \gamma \boldsymbol{x_a} + \mathbf{A}(\boldsymbol{x_h} - \gamma \boldsymbol{x_a}). \quad (2)$$

Note that for a GFIT scaling retrieval, the kernels are calculated for the solution mole fraction profile, not the a priori profile, so the point of linearization of the Taylor expansion producing Eq. (2) is $\gamma \boldsymbol{x_a}$ and not $\boldsymbol{x_a}$.

Table 3. Aircraft overflights. The TCCON site, location and altitudes are listed below, as are the aircraft campaign name, dates and molecules measured and used in this study. In most cases, H_2O radiosonde profiles were measured along with the aircraft campaign, and those are listed separately in column 5, along with the radiosonde type. Column 6 lists the altitude range of the aircraft profiles.

Site	Location	Aircraft campaign	Dates	Species	Altitudes
Park Falls	45.9 N, 90.3 W 0.44 km	INTEX-NA COBRA-ME START-08/pre-HIPPO	12, 15 Jul 2004 15 Jul; 14, 15 Aug 2004 12 May 2008	CO_2, CH_4 CO_2, CO CO_2, CO, CH_4, N_2O, H_2O	0.6–10 km 0.7–(8–10) km 1.2–9 km
Darwin	12.4S, 130.9 E 0.03 km	TWP-ICE	4 Feb 2006	CO_2 H_2O (RS92-15 Vaisala)	0.9–14 km
Lamont	36.6 N, 97.5 W 0.32 km	HIPPO Lear	30 Jan 2009 31 Jul; 2, 3 Aug 2009	CO_2, CO, CH_4, N_2O, H_2O CO_2, CO, CH_4, N_2O H_2O (RS92-KL Vaisala)	0.4–13 km 0.3–13 km
Lauder	45.0 S, 169.7 E 0.37 km	HIPPO	21 Jan 2009	CO_2, CO, CH_4, N_2O, H_2O H_2O (RS92 Vaisala)	0.6–14.5 km
Tsukuba	36.1N, 140.1 E 0.03 km	Beechcraft King Air 200T	7, 15 Jan 2009	CO_2, CH_4 H_2O (RS2-91 Meisei Electric)	0.5–7 km

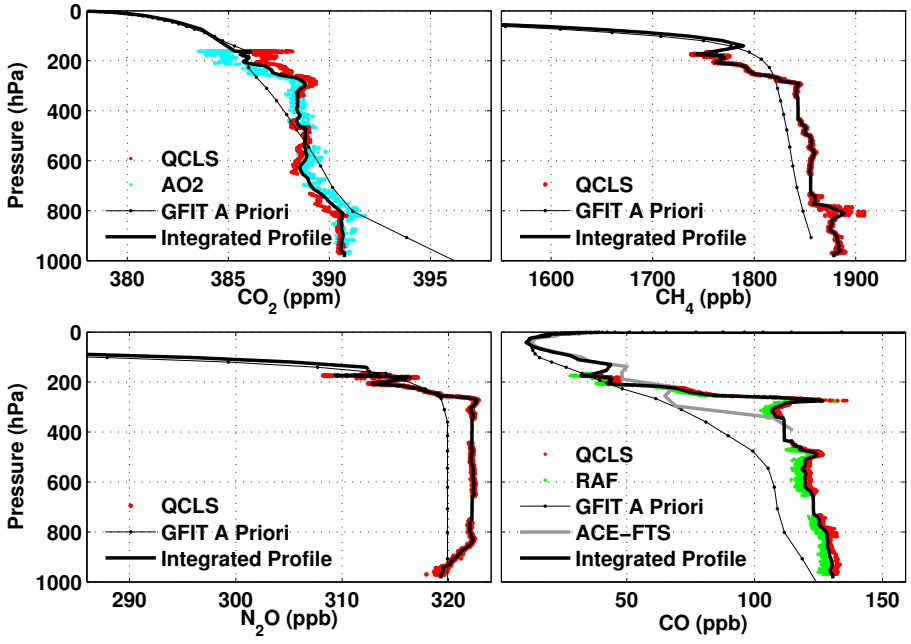

Fig. 2. Lamont profiles from the 30 January 2009 HIPPO overpass. The colored dots show the aircraft data. The thick grey line in the CO panel shows the mean ACE-FTS CO profile. The thin black lines show the GFIT a priori profile for 30 January 2009 over Lamont. The thick black line is the profile that is integrated.

For column measurement calibration, Eq. (2) is integrated vertically:

$$\hat{c}_s = \gamma c_a + \boldsymbol{a}^T(\boldsymbol{x_h} - \gamma \boldsymbol{x_a}) \quad (3)$$

where $\hat{c}_s$ is the smoothed column-averaged DMF, c_a is the column-averaged DMF from integrating the a priori profile and $\boldsymbol{a}$ is a vector containing the FTS dry pressure-weighted column averaging kernel (plotted in Fig. 3). The $\boldsymbol{a}^T(\boldsymbol{x_h} - \gamma \boldsymbol{x_a})$ term represents the column averaging kernel-weighted vertical integration of the difference between the in situ profile and the scaled a priori profile. Column averaging kernels vary as a function of pressure and solar zenith angle.

Integrating these profiles is done most accurately on a pressure grid, under the assumption that the atmosphere

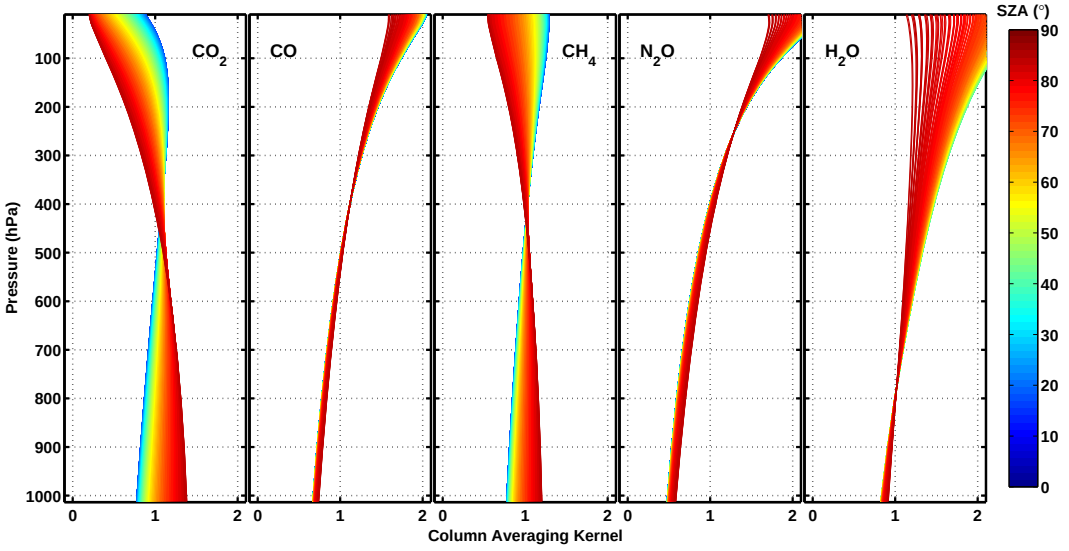

Fig. 3. Column averaging kernels for the Lamont TCCON site. The colors represent different solar zenith angles. Column averaging kernels for other TCCON sites are similar.

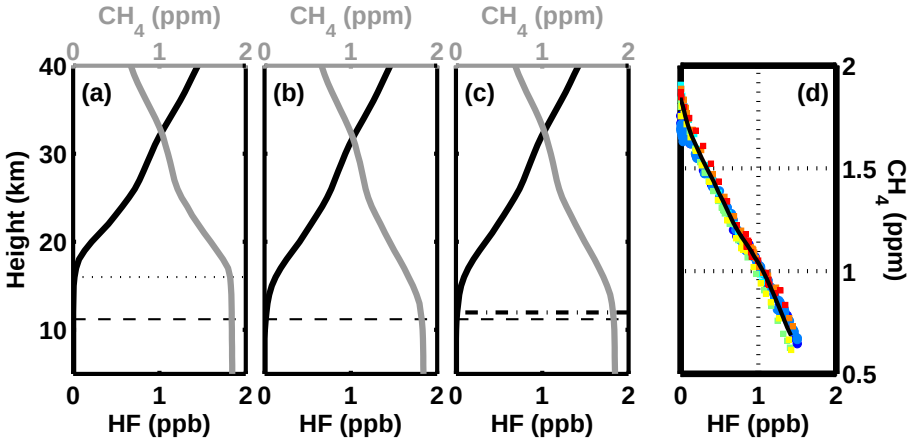

Fig. 4. An illustration of the HF correction used to determine the best stratospheric profiles. Panel **(a)** shows the MkIV FTS balloon profiles before correcting with the NCEP tropopause pressure. The tropopause height for the balloon profiles is indicated with the horizontal dotted line. Panel **(b)** shows the standard GFIT a priori profiles, which uses the NCEP tropopause height (indicated by the horizontal dashed line), pressure, temperature and altitude to scale the gas profiles. Panel **(c)** shows the adjusted GFIT a priori profiles, using the scale factors from the retrieved HF columns. The thick black dash-dot line shows the altitude shift (0.8 km) from an HF scale factor of 0.9. The correlation between HF and CH_4, shown in Panel **(d)**, is preserved for all panels. The blue circles in Panel (d) are from ACE-FTS median profiles from 30–40 N and 30–40 S, ranging from 5–40 km. The squares are from MkIV balloon flights in Septembers of 2003, 2004, 2005 and 2007 from Fort Sumner (34 N, 104 W), also from 5–40 km. The thick black curve is the a priori profile for the TCCON retrievals.

is in hydrostatic balance. The total vertical column for gas G (VC_G) is then defined in the following manner:

$$VC_G = \int_0^{P_s} \frac{f_G(p)}{g \cdot m} dp \tag{4}$$

where $f_G = f_G^{dry} \cdot (1 - f_{H_2O})$ is the true mole fraction of gas G, P_s is the surface pressure, and g is the gravitational acceleration, which is a function of altitude (z) and latitude (ϕ). We distinguish between the true mole fraction (f_G), and the dry mole fraction (f_G^{dry}), which is what the aircraft in situ instrumentation measures. The mean molecular weight of air, m, can be expressed in terms of its wet and dry components as well: $m = m_{H_2O} \cdot f_{H_2O} + m_{air}^{dry} \cdot (1 - f_{H_2O})$. Substituting these into Eq. (4) and rearranging yields a useful, numerically integrable relationship to compute VC_G.

$$VC_G = \int_0^{P_s} \frac{f_G^{dry}(p)}{g(z(p),\phi) \cdot m_{air}^{dry} \cdot \left[1 + f_{H_2O}^{dry}(p) \cdot (m_{H_2O}/m_{air}^{dry})\right]} dp \tag{5}$$

where $f_{\mathrm{G}}^{\mathrm{dry}}$ is the aircraft profile of gas G, $f_{\mathrm{H_2O}}^{\mathrm{dry}} \equiv \frac{f_{\mathrm{H_2O}}}{1-f_{\mathrm{H_2O}}}$, where $f_{\mathrm{H_2O}}$ is the H_2O aircraft or sonde profile, $m_{\mathrm{H_2O}} = 18.02 \times 10^{-3}/N_{\mathrm{A}}$ kg/molecule, $m_{\mathrm{air}}^{\mathrm{dry}} = 28.964 \times 10^{-3}/N_{\mathrm{A}}$ kg/molecule, and N_{A} is Avogadro's constant. To compute the column averaging kernel-weighted vertical column (to satisfy the right-hand term in Eq. 3), the column averaging kernel ($a(p)$) must be included at every level in the integral.

$$VC_{G,ak} = \int_0^{P_{\mathrm{s}}} \frac{f_{\mathrm{G}}^{\mathrm{dry}}(p) \cdot a(p)}{g(z(p),\phi) \cdot m_{\mathrm{air}}^{\mathrm{dry}} \cdot \left[1 + f_{\mathrm{H_2O}}^{\mathrm{dry}}(p) \cdot (m_{\mathrm{H_2O}}/m_{\mathrm{air}}^{\mathrm{dry}})\right]} dp \quad (6)$$

The column of dry air (VC_{air}) is computed by setting the numerator in Eq. (6) to 1. The column-averaged DMF is computed by dividing the appropriate vertical columns by the column of dry air. Hence, Eq. (3) becomes:

$$\hat{c}_{\mathrm{s}} = \gamma c_{\mathrm{a}} + \left(\frac{VC_{G,ak}^{\mathrm{aircraft}} - \gamma VC_{G,ak}^{\mathrm{a\ priori}}}{VC_{\mathrm{air}}} \right) \quad (7)$$

Aircraft measurements have good accuracy, but are limited in altitude floor and ceiling, and so we must use additional information for the surface and the stratosphere. When multiple instruments aboard the aircraft measure the same species, a running mean is applied. There is one instance where two CO measurements on HIPPO-1 disagree over Lauder in the upper troposphere (RAF and QCLS): in this case, QCLS is used.

Most TCCON sites are co-located with tower or surface in situ measurements. In the event that there were no surface or tower measurements available, and the aircraft did not measure down to the surface, the lowest measured aircraft value was assumed to be the surface value (e.g. Park Falls on 14 July 2004).

In general, the unknown state of the atmosphere above the aircraft ceiling is the largest source of uncertainty in the total integrated column (Table 4). For stratospheric CO_2, the mole fractions are predictable at the 0.3% level. The CO_2 profiles in the stratosphere are empirically derived from in situ measurements on high-altitude balloons and include realistic latitude and time-dependencies. The stratosphere is set by an exponential decrease above the tropopause, based on the age of air measurements of Andrews et al. (2001). The tropopause pressure comes from the NCEP/NCAR four-times daily analysis, which is interpolated to local noon at the latitude and longitude of the site. A generous error of ± 1 ppm is assumed for the GFIT stratospheric a priori profile. These stratospheric profiles are used as a priori information for all TCCON retrievals. A priori profiles for the troposphere are derived from GLOBALVIEW (GLOBALVIEW-CO_2, 2006).

Stratospheric N_2O and CH_4 mole fractions are more difficult to estimate than CO_2 because they decrease rapidly with altitude, causing transport-driven variations in the stratospheric column. To account for these transport-driven variations, columns of HF can be used, which are measured coincidently with N_2O and CH_4 by the TCCON FTS instruments. Due to a complete absence of HF in the troposphere, HF is a sensitive indicator of ascent and descent in the stratosphere. Indeed, a 1 km vertical shift in the HF profile produces a $\sim$15% change in the total column, which is easily measureable. Furthermore, strong stratospheric CH_4-HF and N_2O-HF correlations have been observed globally by Luo et al. (1995) and Washenfelder et al. (2003), which we exploit in this analysis to determine the best stratospheric profile for a given overpass.

The GFIT CH_4, N_2O, CO and HF a priori profiles are generated from MkIV FTS balloon profiles (Toon, 1991). The profiles are shifted up or down in altitude depending on the tropopause pressure for local noon on that day. The CH_4-HF and N_2O-HF correlations in the a priori profiles are consistent with those observed by Luo et al. (1995) and Washenfelder et al. (2003) and are preserved under the vertical shifting. Since HF is a long-lived, stable stratospheric tracer, we assume that any difference in the retrieved HF column from the a priori value is due to the stratospheric dynamics and will be anti-correlated with the stratospheric N_2O and CH_4. The magnitude of the deviation of the HF column from the a priori HF column is used to adjust the CH_4 and N_2O stratospheric profiles to generate our best estimate of the "true" stratospheric profile for a given overpass. An illustration of this is in Fig. 4. The average adjustment is 0.4 km, and the maximum adjustment is 1.8 km. Note that even small errors in the stratospheric a priori profile of N_2O will be very important in this analysis, because the N_2O column averaging kernels increase significantly in the stratosphere (Fig. 3). The stratospheric error contribution for both CH_4 and N_2O is estimated by shifting the stratospheric profile up and down by 1 km and integrating the results, giving upper and lower bounds on the column due to errors in the stratospheric profile.

Unlike CH_4 and N_2O, stratospheric CO is highly variable and does not have a simple relationship with HF. To estimate the CO stratospheric contributions, v2.2 profiles from the low-Earth orbiting ACE-FTS instrument (Bernath et al., 2005) were averaged within one month of the overpass and ± 5 degrees latitude of the site. The work by Clerbaux et al. (2008) has shown that the ACE-FTS CO values are accurate to 30% in the upper troposphere/lower stratosphere, and 25% above. For our stratospheric error budget, we have taken the larger of the standard deviation of the ACE profiles and the estimated error by Clerbaux et al. (2008), and summed that in quadrature with shifting the stratospheric profile up and down by 1 km.

If water vapor profiles are not available from the aircraft in situ data (Tsukuba, Darwin and during the Learjet overpasses of Lamont), radiosonde measurements of H_2O are used in Eqs. (5) and (6). Any additional stratospheric information is provided from GFIT a priori profiles, which are derived

Table 4. Aircraft integration error budget. The mean errors (minimum, maximum errors) for the various overpasses indicate the contribution of the error source to the error in the integrated total column. The error is split into three sources: the contribution from the unknown stratospheric profile, the contribution from the unknown surface value (if applicable), and the contribution from the aircraft profile itself. The total error is the sum, in quadrature, of the three errors. The stratospheric error for CO_2 was estimated from a sum, in quadrature, of the errors from shifting the a priori stratospheric profile up by 1 km, and adding 0.3% error to the stratospheric profile. The stratospheric CO contribution was estimated by shifting the stratospheric profile by 1 km and adding 25% error to the stratospheric profile (due to the ACE-FTS profile uncertainty). For CH_4 and N_2O, only the contribution of shifting the stratospheric a priori by 1 km is included. The surface contribution to the error in the total column is generally negligible, since most of these overpasses either had coincident surface in situ measurements available, or reached very close to the surface themselves. The aircraft error was estimated by adding twice the precision of the aircraft measurement to the profile and re-integrating the profile.

Molecule	Stratospheric Error	Surface Error	Aircraft Error	Total Error
CO_2	0.3 ppm (0.1, 0.5)	0.03 ppm (0, 0.2)	0.3 ppm (0.1, 0.7)	0.4 ppm (0.2, 0.8)
CO	3 ppb (1, 5)	0.04 ppb (0.01, 0.08)	4 ppb (1, 8)	5 ppb (2, 9)
CH_4	10 ppb (7, 14)	0.1 ppb (0.02, 0.3)	3 ppb (1.5, 6)	10 ppb (7, 15)
N_2O	4 ppb (4, 5)	0.02 ppb (0, 0.09)	0.4 ppb (0.3, 0.8)	4 ppb (4, 5)

Table 5. TCCON scale factors. The TCCON data are divided by the scale factors to calibrate to the WMO scale. Columns 5 and 6 describe the uncertainties associated with each species, and the WMO-recommended inter-network comparabilities. There are no WMO recommendations for H_2O.

Molecule	Scale factor (TCCON/Aircraft)	Best fit standard error	TCCON:Aircraft ratio uncertainty (2σ)	Species uncertainty (2σ)	WMO recommendation
CO_2	0.989	0.001	0.002	0.8 ppm	0.1 ppm
CO	0.98	0.02	0.04	4 ppb	2 ppb
CH_4	0.978	0.002	0.004	7 ppb	2 ppb
N_2O	0.958	0.005	0.01	3 ppb	0.1 ppb
H_2O	1.03	0.01	0.1	0.4 ppth	–

from NCEP profiles, and extended upwards using a model based on MkIV balloon profiles. Because most of the water column is located at altitudes below ∼5 km, errors in the upper altitude water profile do not significantly affect the total columns of CO_2, CH_4, N_2O and CO.

To estimate the H_2O calibration curve for the TCCON, the radiosonde profiles over Tsukuba, Darwin, Lamont, Lauder and Park Falls are used, which tend to reach higher altitudes than the aircraft (generally well above the tropopause). Water profiles are available from daily sonde measurements at Lamont and Darwin. The errors on the H_2O columns are estimated to be ±5% of the total column.

Once full profiles of the gas of interest and H_2O are generated on a fine altitude or pressure grid, the profiles are integrated via Eqs. (5) or (6), and the smoothed profile is computed via Eq. (7).

5 Results

Aircraft overflights of the Park Falls, Darwin, Lamont, Lauder and Tsukuba TCCON stations are listed in Table 3, including their dates and which molecules were measured on the aircraft. Sample profiles from the HIPPO aircraft over Lamont are shown in Fig. 2 and the derived column-average calibration data are shown in Figs. 5–9. Errors computed for the smoothed, integrated aircraft measurements are the sum in quadrature of estimated stratospheric and surface measurement uncertainties and the estimated error on the aircraft or sonde profiles in the troposphere (Table 4). In all cases (except H_2O), the stratospheric uncertainty is a significant component of the total error. The slopes of the calibration curves are listed in Table 5. Errors on the slopes are quoted as standard errors on the best fit, calculated using the errors in both the x and y axis (York et al., 2004) and as 2 standard deviations of the individual measurement ratios.

Our retrieval method is predicted to be both linear and have no intercept. We thus fit the data with a linear least-squares and force a zero intercept. When the least-squares fits are allowed a nonzero y-intercept, all have a y-intercept that is zero within the uncertainty. To attempt to remove any biases added from errors in the GFIT a priori information, the aircraft profile with our best estimate of the stratospheric profile was input as the a priori profile. The same spectra

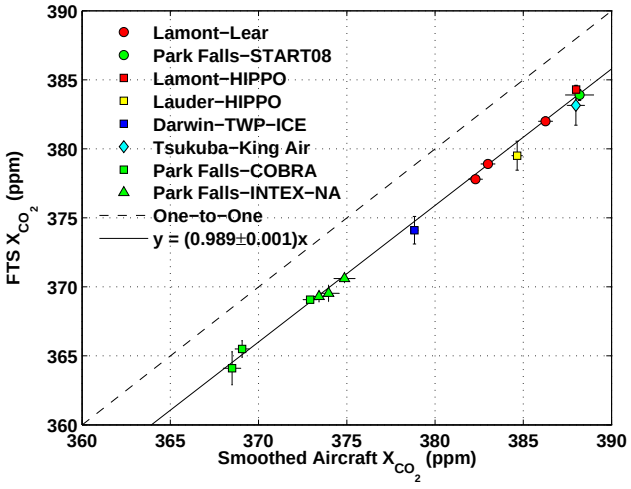

Fig. 5. The TCCON calibration curve for CO_2. The smoothed aircraft value is $\hat{c}_s$ from Eq. (7).

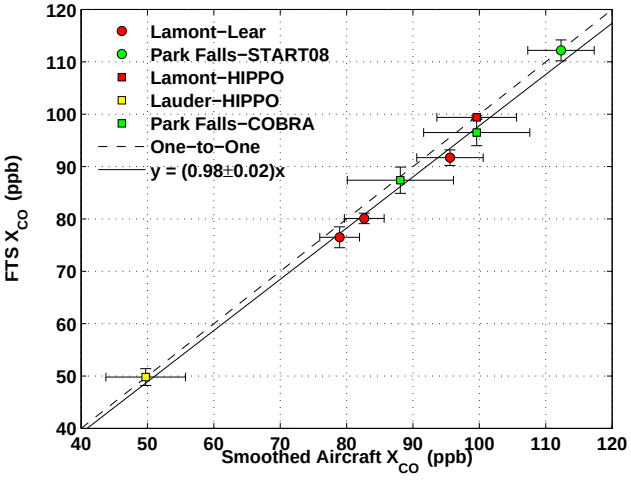

Fig. 6. As in Fig. 5, but for CO.

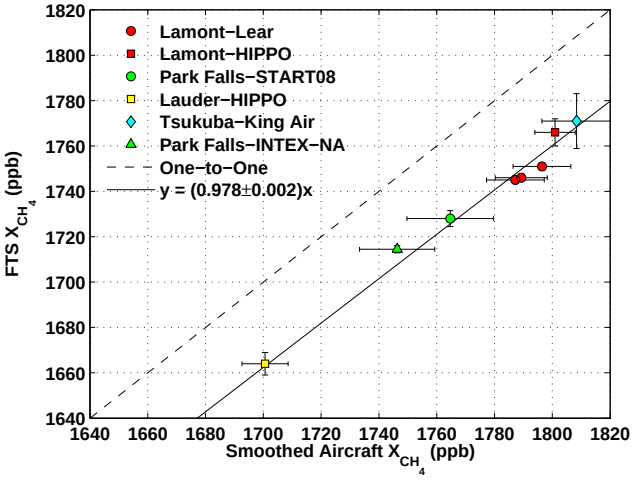

Fig. 7. As in Fig. 5, but for CH_4.

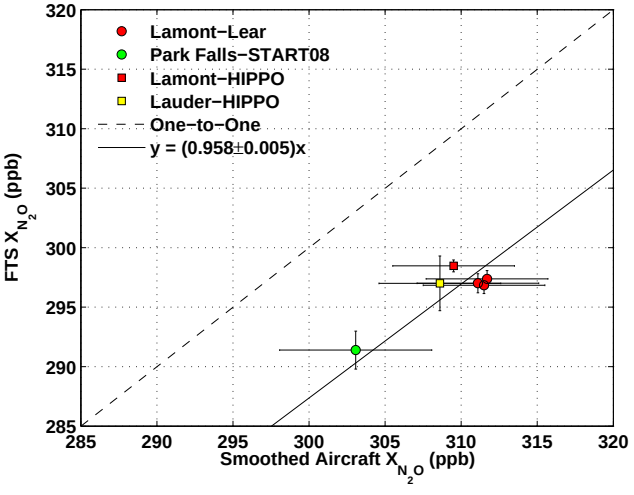

Fig. 8. As in Fig. 5, but for N_2O.

were processed using the standard GFIT a priori profiles as well. The calibration coefficient for both cases have identical slopes within standard error, suggesting that the GFIT a priori profiles do not add a significant bias to the retrievals. Figures 5–9 show the calibration curves calculated using the aircraft profile as the a priori profiles.

For all molecules, there is excellent consistency between the TCCON calibrations obtained from different sites and seasons. Within measurement error, all stations can be described by a single regression line and hence single calibration factor, with variations around the regression line being explicable by instrumental and site differences. Hence, the reported TCCON columns are produced by dividing the retrieved columns by the values listed in Table 5. With the exception of H_2O, all the calibration values are <1. This is because the O_2 spectroscopy has an error that causes the O_2 columns to be ~2% high. The largest uncertainties in the calibration coefficients are for H_2O. The H_2O calibration curve shows that over a large range of humidities, the FTS instruments are capable of measuring water columns to a good degree of accuracy, but due to the high variability of tropospheric H_2O, we do not expect calibration errors as small as for CO_2, CH_4, CO or N_2O.

The uncertainties on the slopes, listed in Table 5, are used to compute the species uncertainty of each molecule, and can be compared with the WMO-recommended intercomparability for the molecules (WMO, 2007). The calibrated TCCON data, though less precise and accurate than the in situ data, provide long time series of total column measurements of atmospheric CO_2, CH_4, CO and N_2O.

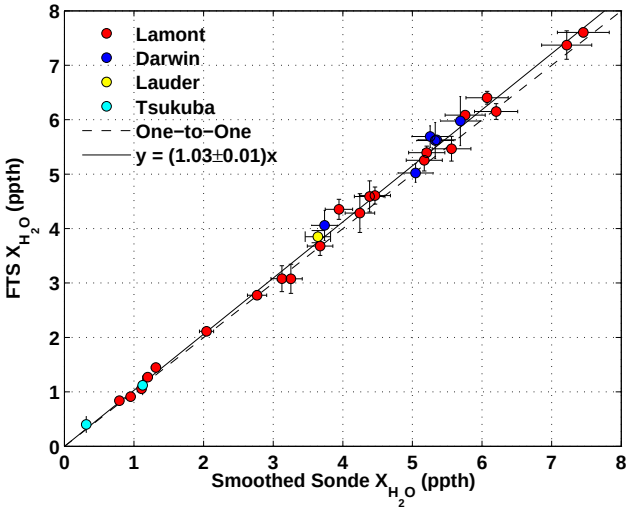

Fig. 9. As in Fig. 5, but for H_2O.

6 Conclusions

The TCCON column-averaged dry-air mole fractions of CO_2, CO, CH_4 and N_2O have been calibrated to the WMO scale using aircraft profiles measured between 2004 and 2009. The TCCON H_2O columns have been calibrated using radiosonde measurements. The calibration curves show excellent consistency between the different TCCON sites and seasons, and can be described by a single calibration factor for each molecule. Future plans include extending this calibration set using additional HIPPO campaigns and other aircraft programs. We expect that all TCCON sites will eventually be calibrated using WMO-scale in situ measurements.

Acknowledgements. The authors wish to thank Stephanie Vay and Donald R. Blake for guidance and the use of the INTEX-NA CO_2 and CH_4 profiles, respectively. The INTEX-NA data were downloaded from ftp://ftp-air.larc.nasa.gov/pub/INTEXA/DC8_AIRCRAFT/ on 10 September 2010. NCEP Reanalysis data is provided by the NOAA/OAR/ESRL PSD, Boulder, Colorado, USA, from their Web site at http://www.cdc.noaa.gov/. Data were obtained through the Atmospheric Radiation Measurement (ARM) Program sponsored by the US Department of Energy, Office of Science, Office of Biological and Environmental Research. Data were generated by the National Oceanic and Atmospheric Administration (NOAA), Earth System Research Laboratory (ESRL), Carbon Cycle Greenhouse Gases Group, including flask data from Andrews et al. (2009). The Meteorological Research Institute tower measurements are described by Inoue and Matsueda (1996). US funding for TCCON comes from NASA's Terrestrial Ecology Program, the Orbiting Carbon Observatory project and the DOE/ARM Program. Part of this work was performed at the Jet Propulsion Laboratory, California Institute of Technology, under contract with NASA. ACE is funded primarily by the Canadian Space Agency. Support for the Learjet-25 measurements was provided by the NASA ASCENDS development and ESTO IIP programs. Support for the flask measurements at the SGP ARM site is from LBNL-DOE contract DE-AC02-05CH11231. We acknowledge funding for Darwin and Wollongong from the Australian Research Council, Projects DP0879468 and LP0562346 with the Australian Greenhouse Office. The National Center for Atmospheric Research is sponsored by the National Science Foundation.

Edited by: H. Worden

References

Abshire, J. B., Riris, H., Allan, G. R., Weaver, C., Mao, J., Sun, X., and Hasselbrack, W.: Pulsed Airborne Lidar Measurements of Atmospheric CO_2 Column Absorption from 3-13 km Altitudes, in: 25th International Laser Radar Conference, 2010.

Andrews, A., Boering, K., Daube, B., Wofsy, S., Loewenstein, M., Jost, H., Podolske, J., Webster, C., Herman, R., Scott, D., et al.: Mean ages of stratospheric air derived from in situ observations of CO_2, CH_4, and N_2O, J. Geophys. Res.-Atmos., 106, 32295–32314, 2001.

Andrews, A., Kofler, J., Bakwin, P., Zhao, C., and Tans, P.: Carbon Dioxide and Carbon Monoxide Dry Air Mole Fractions from the NOAA ESRL Tall Tower Network, 1992–2009, Version: 2010-03-29, ftp://ftp.cmdl.noaa.gov/ccg/towers/, 2009.

Bender, M. L., Battle, M., and Keeling, R. F.: The O_2 Balance of the Atmosphere: A Tool for Studying the Fate of Fossil-Fuel CO_2, Annual Review of Energy and the Environment, 23, 207–223, doi:10.1146/annurev.energy.23.1.207, 1998.

Bernath, P., McElroy, C., Abrams, M., Boone, C., Butler, M., Camy-Peyret, C., Carleer, M., Clerbaux, C., Coheur, P., Colin, R., et al.: Atmospheric chemistry experiment (ACE): mission overview, Geophys. Res. Lett, 32, L15S01, doi:10.1029/2005GL022386, 2005.

Clerbaux, C., George, M., Turquety, S., Walker, K. A., Barret, B., Bernath, P., Boone, C., Borsdorff, T., Cammas, J. P., Catoire, V., Coffey, M., Coheur, P.-F., Deeter, M., De Mazière, M., Drummond, J., Duchatelet, P., Dupuy, E., de Zafra, R., Eddounia, F., Edwards, D. P., Emmons, L., Funke, B., Gille, J., Griffith, D. W. T., Hannigan, J., Hase, F., Höpfner, M., Jones, N., Kagawa, A., Kasai, Y., Kramer, I., Le Flochmoën, E., Livesey, N. J., López-Puertas, M., Luo, M., Mahieu, E., Murtagh, D., Nédélec, P., Pazmino, A., Pumphrey, H., Ricaud, P., Rinsland, C. P., Robert, C., Schneider, M., Senten, C., Stiller, G., Strandberg, A., Strong, K., Sussmann, R., Thouret, V., Urban, J., and Wiacek, A.: CO measurements from the ACE-FTS satellite instrument: data analysis and validation using ground-based, airborne and spaceborne observations, Atmos. Chem. Phys., 8, 2569–2594, doi:10.5194/acp-8-2569-2008, 2008.

Deutscher, N. M., Griffith, D. W. T., Bryant, G. W., Wennberg, P. O., Toon, G. C., Washenfelder, R. A., Keppel-Aleks, G., Wunch, D., Yavin, Y., Allen, N. T., Blavier, J.-F., Jimnez, R., Daube, B. C., Bright, A. V., Matross, D. M., Wofsy, S. C., and Park, S.: Total column CO_2 measurements at Darwin, Australia – site description and calibration against in situ aircraft profiles, Atmos. Meas. Tech., 3, 947–958, doi:10.5194/amt-3-947-2010, 2010.

Dlugokencky, E., Myers, R., Lang, P., Masarie, K., Crotwell, A., Thoning, K., Hall, B., Elkins, J., and Steele, L.: Conversion of NOAA atmospheric dry air CH_4 mole fractions to a

gravimetrically prepared standard scale, J. Geophys. Res., 110, D18306, doi:10.1029/2005JD006035, 2005.

Frankenberg, C., Warneke, T., Butz, A., Aben, I., Hase, F., Spietz, P., and Brown, L. R.: Pressure broadening in the 2_v3 band of methane and its implication on atmospheric retrievals, Atmos. Chem. Phys., 8, 5061–5075, doi:10.5194/acp-8-5061-2008, 2008.

Gerbig, C., Lin, J., Wofsy, S., Daube, B., Andrews, A., Stephens, B., Bakwin, P., and Grainger, C.: Toward constraining regional-scale fluxes of CO_2 with atmospheric observations over a continent: 2. Analysis of COBRA data using a receptor-oriented framework, J. Geophys. Res, 108, 4757, doi:10.1029/2003JD003770, 2003.

GLOBALVIEW-CO_2: Cooperative Atmospheric Data Integration Project – Carbon Dioxide, CD-ROM, NOAA GMD, Boulder, Colorado, 2006.

Gordon, I. E., Kassi, S., Campargue, A., and Toon, G. C.: First identification of the $a^1\Delta_g - X^3\Sigma_g^-$ electric quadrupole transitions of oxygen in solar and laboratory spectra, J. Quant. Spectrosc. Ra. , 111, 1174–1183, 2010.

Hall, B., Dutton, G., and Elkins, J.: The NOAA nitrous oxide standard scale for atmospheric observations, J. Geophys. Res, 112, D09305, doi:10.1029/2006JD007954, 2007.

Inoue, H. and Matsueda, H.: Variations in atmospheric CO_2 at the Meteorological Research Institute, Tsukuba, Japan, J. Atmos. Chem., 23, 137–161, 1996.

Jenouvrier, A., Daumont, L., Régalia-Jarlot, L., Tyuterev, V. G., Carleer, M., Vandaele, A. C., Mikhailenko, S., and Fally, S.: Fourier transform measurements of water vapor line parameters in the 4200–6600 cm^{-1} region, J. Quant. Spectrosc. Ra., 105, 326–355, 2007.

Keeling, C., Guenther, P., Emanuele III, G., Bollenbacher, A., and Moss, D.: Scripps reference gas calibration system for carbon dioxide-in-nitrogen and carbon dioxide-in-air standards: Revision of 1999 (with addendum), Tech. rep., SIO Reference Series No. 01-11, http://scrippsco2.ucsd.edu/publications/refgas_report_2002.pdf, 2002.

Keppel-Aleks, G., Wennberg, P., Schneider, T., Honsowetz, N., and Vay, S.: Total column constraints on Northern Hemisphere carbon dioxide surface exchange, in: American Geophysical Union, Fall Meeting 2008, abstract #A43F-03, 2008.

Lin, J. C., Gerbig, C., Wofsy, S. C., Daube, B. C., Matross, D. M., Chow, V. Y., Gottlieb, E., Andrews, A. E., Pathmathevan, M., and Munger, J. W.: What have we learned from intensive atmospheric sampling field programs of CO_2?, Tellus B, 58, 331–343, 2006.

Luo, M., Cicerone, R., and Russell, J.: Analysis of Halogen Occultation Experiment HF versus CH_4 correlation plots: chemistry and transport implications, J. Geophys. Res., 100, 13927–13937, 1995.

Machida, T., Katsumata, K., Tohjima, Y., Watai, T., and Mukai, H.: Preparing and maintaining of CO2 calibration scale in National Institute for Environmental Studies-NIES 95 CO2 scale, in: Report of the 14th WMO Meeting of Experts on Carbon Dioxide Concentration and Related Tracer Measurement Techniques, Helsinki, Finland, 10–13, 2007.

Machida, T., Matsueda, H., Sawa, Y., Nakagawa, Y., Hirotani, K., Kondo, N., Goto, K., Nakazawa, T., Ishikawa, K., and Ogawa, T.: Worldwide Measurements of Atmospheric CO2 and Other Trace Gas Species Using Commercial Airlines, J. Atmos. Ocean. Tech., 25, 1744–1754, doi:10.1175/2008JTECHA1082.1, 2008.

May, P., Mather, J., Vaughan, G., Jakob, C., McFarquhar, G., Bower, K., and Mace, G.: The tropical warm pool international cloud experiment, B. Am. Meteorol. Soc., 89, 629–645, 2008.

Novelli, P., Collins, Jr., J., Myers, R., Sachse, G., and Scheel, H.: Reevaluation of the NOAA/CMDL carbon monoxide reference scale and comparisons with CO reference gases at NASA-Langley and the Fraunhofer Institut, J. Geophys. Res., 99, 12833–12839, 1994.

Pan, L. L., Bowman, K. P., Atlas, E. L., Wofsy, S. C., Zhang, F., Bresch, J. F., Ridley, B. A., Pittman, J. V., Homeyer, C. R., Romashkin, P., and Cooper, W. A.: The Stratosphere-Troposphere Analyses of Regional Transport 2008 Experiment, B. Am. Meteorol. Soc., 91, 327–342, doi:10.1175/2009BAMS2865.1, 2010.

Rodgers, C. and Connor, B.: Intercomparison of remote sounding instruments, J. Geophys. Res, 108, 4116–4229, 2003.

Rothman, L., Gordon, I., Barbe, A., Benner, D., Bernath, P., Birk, M., Boudon, V., Brown, L., Campargue, A., Champion, J., et al.: The HITRAN 2008 molecular spectroscopic database, J. Quant. Spectrosc. Ra., 110, 533–572, 2009.

Singh, H., Brune, W., Crawford, J., Jacob, D., and Russell, P.: Overview of the summer 2004 Intercontinental Chemical Transport Experiment-North America (INTEX-NA), J. Geophys. Res. Atmos., 111, D24S01, doi:10.1029/2006JD007905, 2006.

Smith, K. and Newnham, D.: Near-infrared absorption cross sections and integrated absorption intensities of molecular oxygen(O_2, O_2-O_2, and O_2-N_2), J. Geophys. Res., 105, 7383–7396, 2000.

Sussmann, R., Borsdorff, T., Rettinger, M., Camy-Peyret, C., Demoulin, P., Duchatelet, P., Mahieu, E., and Servais, C.: Technical Note: Harmonized retrieval of column-integrated atmospheric water vapor from the FTIR network – first examples for long-term records and station trends, Atmos. Chem. Phys., 9, 8987–8999, doi:10.5194/acp-9-8987-2009, 2009.

Tanaka, T., Morino, I., Machida, T., Kojima, H., Yamaguchi, K., amd Emi Ota, T. K., Oyama, H., Oguma, H., Uchino, O., and Yokota, T.: Aircraft Measurement of Carbon Dioxide for Calibration of Ground-Based High-Resolution Fourier Transform Spectrometer at Tsukuba, in: 8th International Carbon Dioxide Conference, 13–19 September, Jena, Germany, 2009.

Tohjima, Y., Machida, T., Watai, T., Akama, I., Amari, T., and Moriwaki, Y.: Preparation of gravimetric standards for measurements of atmospheric oxygen and reevaluation of atmospheric oxygen concentration, J. Geophys. Res. Atmos., 110, D11302, doi:10.1029/2004JD005595, 2005.

Toon, G.: The JPL MkIV interferometer, Optics Photonics News, 2, 19–21, 1991.

Toth, R.: Measurements of positions, strengths and self-broadened widths of H_2O from 2900 to 8000 cm^{-1}: line strength analysis of the 2nd triad bands, J. Quant. Spectrosc. Ra., 94, 51–107, 2005.

Toth, R., Brown, L., Miller, C., Malathy Devi, V., and Benner, D.: Spectroscopic database of CO_2 line parameters: 4300–7000 cm^{-1}, J. Quant. Spectrosc. Ra., 109, 906–921, 2008.

Washenfelder, R., Wennberg, P., and Toon, G.: Tropospheric methane retrieved from ground-based near-IR solar absorption spectra, Geophys. Res. Lett., 30, 2226, doi:10.1029/2003GL017969, 2003.

Washenfelder, R., Toon, G., Blavier, J., Yang, Z., Allen, N., Wennberg, P., Vay, S., Matross, D., and Daube, B.: Carbon

dioxide column abundances at the Wisconsin Tall Tower site, J. Geophys. Res, 111, D22305, doi:10.1029/2006JD007154, 2006.

WMO: 14th WMO/IAEA Meeting of Experts on Carbon Dioxide Concentration and Related Tracers Measurement Techniques, Tech. rep., WMO/IAEA, Helsinki, Finland, http://www.fmi.fi/kuvat/14thExpertsRecom.pdf, 2007.

Wofsy, S. C., Daube, B. C., Jimenez, R., Kort, E., Pittman, J. V., Park, S., Commane, R., Xiang, B., Santoni, G., Jacob, D., Fisher, J., Pickett-Heaps, C., Wang, H., Wecht, K., Wang, Q.-Q., Stephens, B. B., Schertz, S., Romashkin, P., Campos, T., Haggerty, J., Cooper, W. A., Rogers, D., Beaton, S., Elkins, J. W., Fahey, D., Gao, R., Moore, F., Montzka, S. A., Schwartz, J. P., Hurst, D., Miller, B., Sweeney, C., Oltmans, S., Nance, D., Hintsa, E., Dutton, G., Watts, L. A., Spackman, R., Rosenlof, K., Ray, E., Zondlo, M., Diao, M., Mahoney, M. J., Chahine, M., Olsen, E., Keeling, R., Bent, J., Atlas, E. A., Lueb, R., Patra, P., Ishijima, K., Engelen, R., Nassar, R., Jones, D. B., and Mikaloff-Fletcher, S.: HIAPER Pole-to-Pole Observations (HIPPO): Fine grained, global scale measurements for determining rates for transport, surface emissions, and removal of climatically important atmospheric gases and aerosols, Philos. T. R. Soc. A, in press, 2010.

Wunch, D., Wennberg, P., Toon, G., Keppel-Aleks, G., and Yavin, Y.: Emissions of greenhouse gases from a North American megacity, Geophys. Res. Lett., 36, L15810, doi:10.1029/2009GL039825, 2009.

Wunch, D., Toon, G. C., Blavier, J.-F. L., Washenfelder, R., Notholt, J., Connor, B. J., Griffith, D. W. T., Sherlock, V., and Wennberg, P. O.: The Total Carbon Column Observing Network (TCCON), Philos. T. R. Soc. A, in press, 2010.

Yang, Z., Wennberg, P., Cageao, R., Pongetti, T., Toon, G., and Sander, S.: Ground-based photon path measurements from solar absorption spectra of the O_2 A-band, J. Quant. Spectrosc. Ra., 90, 309–321, 2005.

Yang, Z., Washenfelder, R., Keppel-Aleks, G., Krakauer, N., Randerson, J., Tans, P., Sweeney, C., and Wennberg, P.: New constraints on Northern Hemisphere growing season net flux, Geophys. Res. Lett., 34, L12807, doi:10.1029/2007GL029742, 2007.

York, D., Evensen, N., Martínez, M., and Delgado, J.: Unified equations for the slope, intercept, and standard errors of the best straight line, American Journal of Physics, 72, 367, 2004.

Zhao, C. and Tans, P.: Estimating uncertainty of the WMO mole fraction scale for carbon dioxide in air, J. Geophys. Res., 111, D08S09, doi:10.1029/2005JD006003, 2006.

Zhou, L., Kitzis, D., and Tans, P.: 2.3 Report of the Fourth WMO Round-Robin Reference Gas Intercomparison, in: WORKSHOP PROCEEDINGS, p. 40, 2009.

Zondlo, M. A., Paige, M., Massick, S., and Silver, J.: Vertical Cavity Laser Hygrometer for the National Science Foundation Gulfstream-V Aircraft, J. Geophys. Res.-Atmos., doi:10.1029/2010JD014445, in press, 2 August 2010.